



PERGAMON

Geothermics 28 (1999) 161–187

GEOTHERMICS

A geochemical reconnaissance of the Alid volcanic center and geothermal system, Danakil depression, Eritrea

Jacob B. Lowenstern^{a,*}, Cathy J. Janik^a, Robert O. Fournier^a,
Theoderos Tesfai^b, Wendell A. Duffield^c,
Michael A. Clynné^a, James G. Smith^a, Leake Woldegiorgis^d,
Kidane Weldemariam^b, Gabreab Kahsai^b

^a*U.S. Geological Survey, Mail Stop 910, 345 Middlefield Road, Menlo Park, CA 94025 U.S.A.*

^b*Department of Mines, Eritrean Ministry of Energy and Mines, P.O. Box 272, Asmara, Eritrea*

^c*U.S. Geological Survey, 2255 North Gemini Drive, Flagstaff, AZ 86001 U.S.A.*

^d*Department of Energy, Eritrean Ministry of Energy and Mines, P.O. Box 5285, Asmara, Eritrea*

Received 4 March 1998; accepted 14 July 1998

Abstract

Geological and geochemical studies indicate that a high-temperature geothermal system underlies the Alid volcanic center in the northern Danakil depression of Eritrea. Alid is a very late-Pleistocene structural dome formed by shallow intrusion of rhyolitic magma, some of which vented as lavas and pyroclastic flows. Fumaroles and boiling pools distributed widely over an area of $\sim 10 \text{ km}^2$ on the northern half of Alid suggest that an active hydrothermal system underlies much of that part of the mountain. Geothermometers indicate that the fumarolic gases are derived from a geothermal system with temperatures $> 225^\circ\text{C}$. The isotopic composition of condensed fumarolic steam is consistent with these temperatures and implies that the source water is derived primarily from either lowland meteoric waters or fossil Red Sea water, or both. Some gases vented from the system (CO_2 , H_2S and He) are largely magmatic in origin. Permeability beneath the volcanic center may be high, given the amount of intrusion-related deformation and the active normal faulting within the Danakil depression. Published by Elsevier Science Ltd on behalf of CNR. All rights reserved.

Keywords: geochemistry; geothermometry; isotopes; fumaroles; Afar; Eritrea

* Corresponding author: jlwstrn@usgs.gov

1. Introduction

The Danakil depression, or northern Afar triangle, a region of active volcanism and high heat flow, has long been recognized as an area with geothermal potential (UNDP, 1973). Because of its inhospitable climate and difficult access and the recent history of political unrest in the region, the geology and geochemistry of the northern Afar has remained poorly studied.

In 1991, after a 30-year war, Ethiopia relinquished its claim on the land of Eritrea, and the independent State of Eritrea was founded and given international recognition in 1993. Due in part to the war, the country has relatively little infrastructure and many regions are without electricity. The total installed electrical capacity of the country was 35 MW in 1992, for a population of > 3 million.

At the request of the Eritrean government and the U.S. Agency for International Development, a team of ten U.S. and Eritrean geologists and geochemists traveled to the Alid volcanic center in the Danakil depression, about 90 km south of the port of Massawa. The purpose of the expedition was to assess the geothermal potential of Alid through geologic mapping, geochronology and geochemical sampling (Clynne et al., 1996a, 1996b; Duffield et al., 1997). Below, we discuss a variety of chemical, isotopic and geological data to demonstrate that the Alid volcanic center is a promising geothermal target. In addition, we publish some of the first detailed geochemical data for this part of the Danakil area and provide a hydrologic and geochemical framework that may be used as a starting point for further exploration of the region.

2. Geological background

Alid volcanic center, Eritrea, is located along the axis of the Danakil depression, the graben trace of a crustal spreading center that radiates NNW from a plate-tectonic triple junction situated within a complexly rifted and faulted basaltic lowland called the Afar Triangle (Fig. 1). The Danakil depression is a subaerial segment of the spreading system that is opening to form the Red Sea. Crustal spreading along the axis of the Red Sea is transferred to spreading along the Danakil segment in a right-stepping en echelon pattern (Barberi and Varet, 1977). The Danakil segment shows increased opening southeastward to the Afar triple junction. Kinematically, this configuration is consistent with spreading and rotation about a pivot point near the Gulf of Zula, about 40 km NNW of Alid, and can account for the triangular shape of the Afar lowland and anti-clockwise rotation of a horst of basement rock (the Danakil Alps) within the zone of en echelon overlap between the Red Sea and Danakil spreading centers (Souriot and Brun, 1992).

The northern Danakil depression lies near or below sea level for much of its extent. It is surrounded by the Danakil horst (Alps) to the east and the Eritrean plateau or highland to the west, the latter rising to elevations of 2000–3000 m a.s.l. Both of these bordering regions are underlain primarily by Precambrian gneisses, granites and schists, in some places covered by Mesozoic-to-Tertiary sediments and Tertiary basalts. Much of the Afar lowland is covered with Pliocene and Quaternary lavas

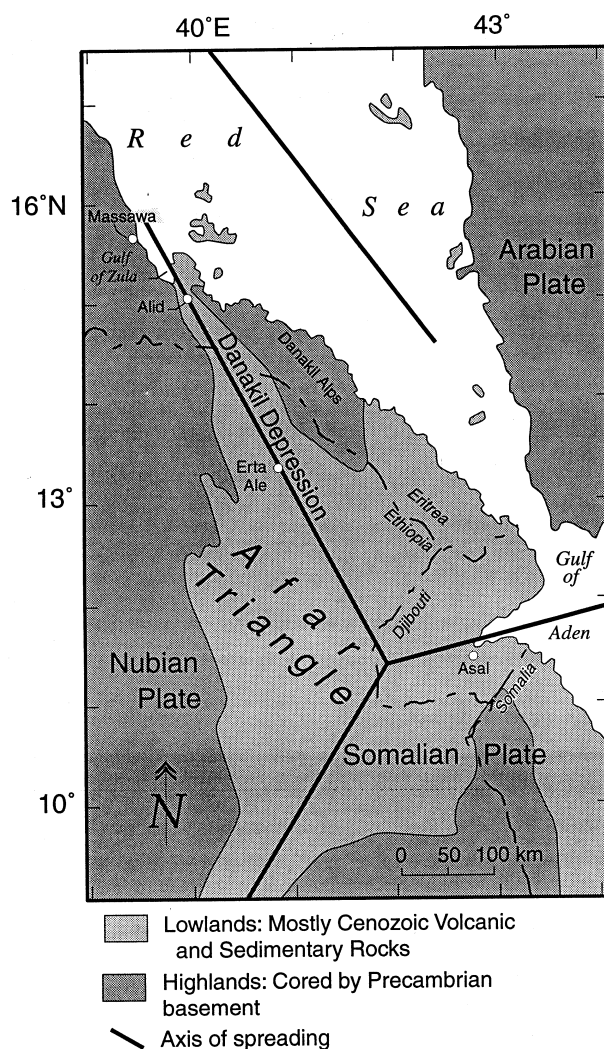


Fig. 1. Simplified plate-tectonic map of the Afar triangle region modified from figures in Barberi and Varet (1977). The Afar triangle corresponds to the lowland area bounded by the Somalian highlands to the south, the Eritrean and Ethiopian highlands to the west and the Red Sea and Danakil Alps to the northeast. Also labeled are Alid volcanic center, the Asal geothermal system, the Erta Ale shield volcano and the city of Massawa.

(CNR-CNRS, 1973). Erta Ale, one of the most active volcanoes in the world, lies about 200 km SE of Alid.

Alid volcanic center itself is an elliptical structural dome that rises as a single mountain, up to 700 m above the flat plains of the Danakil depression, to a summit of 904 m. The dome formed during late-Pleistocene uplift caused by shallow intrusion of rhyolitic magma, some of which erupted. The major axis of the mountain is 7 km,

elongate in an ENE–WSW direction, perpendicular to the trend of the graben (Fig. 2). The minor axis is about 5 km long, parallel to the graben. Alid rises above a field of young basaltic lavas ('Oss basalts' of Marinelli et al., 1980; yb on Fig. 2), the most recent of which lap unconformably against the north and south flanks of the mountain. Marini (1938) noted fumarolic activity at the south end of the southern 'Oss basalt', indicating very recent volcanic activity.

Most of the following geological summary is based on Clynne et al. (1996a, 1996b) and Duffield et al. (1997). The oldest rocks within the Alid structural dome are Precambrian mica and kyanite schists (pc on Fig. 2) that crop out only in a small area exposed in a deep canyon that drains the east side of the mountain. Overlying this basement rock is the 'sedimentary sequence' (ss), consisting of marine siltstones and sandstones, gypsum beds, fossiliferous limestones, pillow basalts and subaerial basalts, all interpreted to be late Pliocene or, more likely, Pleistocene in age. The 'sedimentary sequence' is found on all parts of the mountain, and dips radially away from its geographic center. Stratigraphically above the 'sedimentary sequence' is the 'lava shell' (ls), which consists of basalts, basaltic andesites and some rhyolite. These rocks form most of the dip slopes of the mountain and their dips locally exceed 50°. Such extreme dip slopes must have formed subsequent to emplacement of the fluid mafic lava flows, as they are far too steep to be original.

Up to 1000 m of structural doming, which began less than ~36 ka (Duffield et al., 1997) caused considerable distension of the 'lava shell' and 'sedimentary sequence' and effected landsliding and collapse of the central region of the mountain, resulting in a basin-like depression. This uplift is roughly coincident with the final dessication of the Red Sea in the southern Danakil depression (Bonatti et al., 1971), consistent with uplift events at Alid causing separation of the Red Sea from its southern arm in the Danakil region. Fractures associated with deformation at Alid are apparent on Fig. 6 of Duffield et al. (1997) and are discussed in that reference. A number of pyroxene rhyolite lavas (frhy) were erupted on the flanks of the mountain, subsequent to structural doming, within the past 35 ka. After the dome existed as an eroded structure, similar rhyolite was erupted as pyroclastic deposits (pf) from the depressed-summit region, $\sim 23.5 \pm 1.9$ ka (Duffield et al., 1997).

Within the pyroclastic deposits are lithic clasts of a medium-grained pyroxene granite that is compositionally and isotopically nearly indistinguishable from the rhyolitic pumice (Lowenstern et al., 1997). Instead of a glassy matrix, as in the volcanic rocks, the granite matrix is made up of granophyric intergrowths of quartz and feldspar that surround phenocrysts. Such granophyric intergrowths can form by relatively rapid cooling of shallow igneous bodies (Smith, 1974). We interpret these lithic clasts to be crystallized blocks of the same shallow intrusive body that caused the structural doming of Alid.

The geologic data are consistent with the following interpretation: a shallow (≤ 4 km) body of rhyolitic magma intruded beneath Alid, caused structural doming, and erupted as pyroclastic material. The lack of basaltic vents on Alid that are younger than the pyroclastic deposits, even though such vents are common to the north and south, may signify that silicic magma still resides beneath Alid and impedes the ascent of mafic magma (Bailey et al., 1976; Clynne et al., 1996a, 1996b). Even if the magma

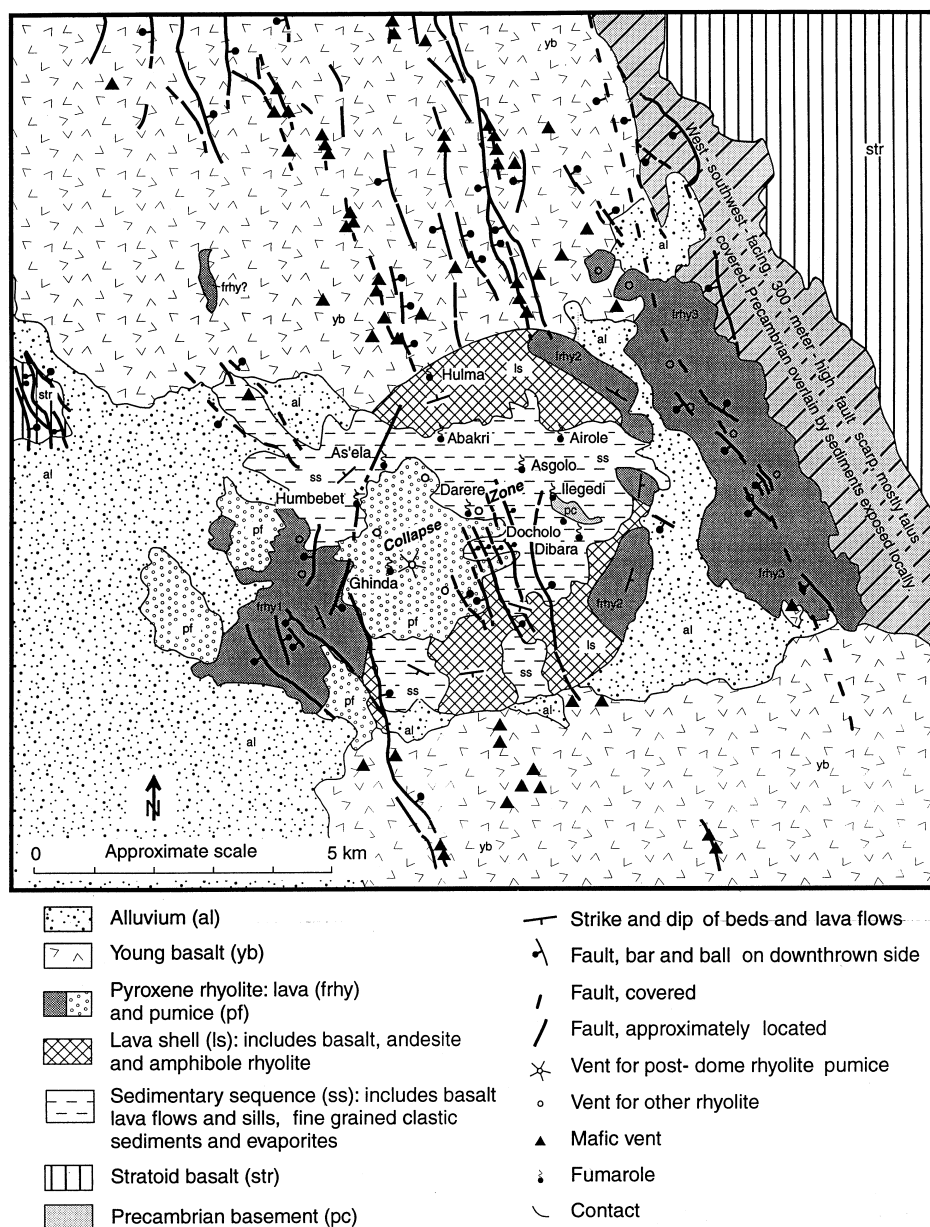


Fig. 2. Generalized geologic map of Alid volcanic center. Because map was traced from lines on air photographs, the scale is approximate and varies somewhat across the illustration. Fumarole sites are labeled.

has since crystallized, it would still remain near its solidus, and represents a likely heat source for the fumaroles of Alid and any associated geothermal system.

3. Regional hydrology and meteorology

Very few data exist regarding the regional groundwater table in the Danakil depression. Given the relative lack of surface waters and wells and the absence of precipitation records for the area, one has to rely partly on geological inferences to piece together a hydrologic interpretation of the Alid geothermal system and its surroundings.

General descriptions of the meteorological characteristics of northeastern Africa, including Eritrea and the Danakil region, have appeared in various publications and reports, including Food and Agriculture Organization (1983), Michael (1986), Eklundh and Pilesji (1990) and Beltrando and Camberlin (1993). Annual rainfall on the central highlands is generally 500–700 mm, and comes from storms propelled by monsoonal winds blowing across Africa from the southwest toward the northeast. This rain occurs mostly in July and August (Eritrea, Government of the State of, 1995). Little, if any, rain falls on the central highlands December through February. The eastern lowlands, the area that includes the Danakil depression and the Red Sea coast of Eritrea, generally receives less than 300 mm per year of rain. Most of this rain falls in December and January from storms associated with monsoonal winds blowing off the Red Sea from the northeast toward the southwest (Eritrea, Government of the State of, 1995). Seasonal and annual variations in rainfall can be very great, particularly in these desert lowland regions. Rainfall there may be very spotty, with no rain falling for a year or more on parts of the lowland region while nearby areas are subjected to brief, torrential downpours.

Rivers and streams flowing to the eastern lowlands from the high plateau disappear into alluvial fan deposits or pond in closed-basin lakes where the water evaporates to form playas. Lenses of relatively fresh and non-evaporated water may pond in the subsurface over deeper bodies of denser brine.

Based on the topographic and geologic setting of Alid, the most likely potential sources of water that could enter its geothermal systems are: (a) fossil Red Sea water that may be present at relatively shallow depths throughout much of the Danakil depression —such waters would have entered the groundwater system the last time that the Red Sea occupied the Danakil depression (32 ka; Bonatti et al., 1971) and today would sit beneath thin, buoyant lenses of fresh-water; (b) local rain that falls on and around Alid; (c) meteoric water that falls on the Eritrean plateau and flows as surface and ground waters toward the eastern lowlands; (d) highly evaporated, high-density brine that accumulates by evaporation of waters that flow into closed basins 15–25 kilometers to the south of Alid; and (e) magmatic fluids from the Alid intrusion and related regional volcanism.

To help determine which of these possible water sources is most likely, we compare stable isotope compositions of geothermal steam with those of different types of water in the Danakil depression as well as adjacent highland and lowland areas.

4. Sample collection and analysis

We used standard collection procedures as outlined in Trujillo et al. (1987), Giggenbach and Goguel (1989) and Fahlquist and Janik (1992). Specific information on collection and analysis for the Alid geothermal samples and Eritrean groundwaters is available in Duffield et al. (1997).

The sulfur in fumarolic H_2S was precipitated as BaSO_4 in Menlo Park and analyzed with a Micromass Optima mass spectrometer by W.C. Pat Shanks of the USGS in Denver, CO. Samples were combusted at 1000°C in the online elemental analyzer and isotope ratios were determined following chromatographic gas cleanup by continuous-flow mass spectrometry. Samples are referenced to Canyon Diablo Troilite (CDT) and precision is $\pm 0.2\text{‰}$. The $\delta^{13}\text{C}$ in CO_2 from fumarolic gases and δD and $\delta^{18}\text{O}$ in steam condensates, spring and surface waters were analyzed in the laboratory of Carol Kendall at the USGS in Menlo Park, CA. Isotopic values are reported relative to Vienna Standard Mean Ocean Water (VSMOW). Analytical precision for $\delta^{18}\text{O}$ is $\pm 0.1\text{‰}$, whereas that for δD is $\pm 2\text{‰}$ and $\delta^{13}\text{C}$ is 0.2‰ . Peter Larson, of Washington State University, analyzed representative rocks for their oxygen isotope compositions according to methods outlined in Larson and Zimmerman (1991). Precision of $\delta^{18}\text{O}$ analysis of oxygen in silicate minerals and rocks is $\pm 0.2\text{‰}$.

5. Groundwaters and surface waters

5.1. Chemistry

Twenty-two water samples from springs, streams and shallow wells were collected in the course of this study (Fig. 3, Table 1). We concentrated on areas from the

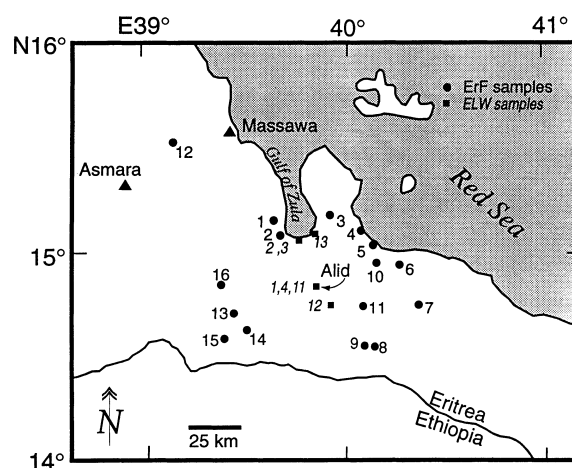


Fig. 3. Map of sampling sites for streams, wells and rainwater. Samples labeled in italics are from the ELW series, whereas normal typefont denotes ErF series of Tables 1 and 2. All samples collected in 1996.

Table 1. Sample information

Sample no	Date in 1996	Name	Latitude (N)	Longitude (E)	Source	Region	Elev. (m)	Temp. (°C)
<i>Regional Waters</i>								
ErF96-1	3-Feb	Kedra Village	15°08'45"	39°38'36"	Drilled well	E lowlands NW of Alid	120	30
ErF96-2	3-Feb	Irafayle	15°04'37"	39°45'00"	Dug well	E lowlands NW of Alid	91	34
ErF96-3	3-Feb	Bordele	15°10'34"	39°55'16"	Dug well	E lowlands N of Alid	150	35
ErF96-4	3-Feb	Ghela'elo	15°06'12"	40°04'36"	Drilled well	E lowlands NE of Alid	130	35
ErF96-5	4-Feb	Akilo	15°01'06"	40°08'45"	Dug well	E lowlands NE of Alid	65	30
ErF96-6	4-Feb	Gorei	14°55'24"	40°15'24"	Drilled well	E lowlands ENE of Alid	95	38
ErF96-7	4-Feb	Adeto	14°44'41"	40°20'55"	Drilled well	E lowlands ESE of Alid	90	37
ErF96-8	4-Feb	Boleli	14°33'07"	40°07'54"	Dug pit	E lowlands SE of Alid	9	34
ErF96-9	4-Feb	Boleli area	14°33'08"	40°05'41"	Stream	E lowlands SE of Alid	67	34
ErF96-10	5-Feb	Adi Ela	14°57'14"	40°07'32"	Drilled well	E lowlands ENE of Alid	120	38
ErF96-11	5-Feb	Somoti I	14°44'04"	40°04'34"	Dug well	E lowlands SE of Alid	61	36
ErF96-12	7-Feb	Near Gahtielay	15°30'38"	39°08'07"	Drilled well	E escarpment	355	42
ErF96-13	8-Feb	Simoli	14°41'35"	39°25'28"	Drilled well	Central highlands	2375	24
ErF96-14	8-Feb	Zegfel (NE of Simoli)	14°36'37"	39°28'05"	Drilled well	Central highlands	2485	24
ErF96-15	8-Feb	Near Ethiopian border	14°34'28"	39°24'01"	Drilled well	Central highlands	2450	28
ErF96-16	8-Feb	Adi-Keyh	14°50'03"	39°22'47"	Dug well	Central highlands	2350	28
ELW96-1	6-Feb	Rain near Boya	14°50'09"	39°51'10"	Rain	E lowlands	300	n.m.
ELW96-2	6-Feb	Gelti hot spring	15°03'39"	39°46'46"	Spring	Gulf of Zula	0	58

ELW96-3	6-Feb	Gerba'naba hot spring	15°03'29"	39°46'27"	Spring	Gulf of Zula	0	54
ELW96-4	7-Feb	Boya	14°49'27"	39°50'40"	Dug well	E lowlands SW of Alid	300	33
ELW96-11	17-Feb	Boya	14°49'27"	39°50'40"	Dug well	E lowlands SW of Alid	300	33
ELW96-12	18-Feb	Alad	14°45'22"	39°56'02"	Stream	E lowlands SE of Alid	30	n.m.
ELW96-13	19-Feb	Kusurale	15°04'07"	39°48'26"	Dug well	E lowlands N of Alid	3	n.m.
<i>Thermal Manifestations of Alid</i>								
<i>Waters</i>								
ELW96-5	10-Feb	Ilegedi #1	14°52'54"	39°55'37"	Bubbling pool	Alid	515	50
ELW96-6	10-Feb	Ilegedi #2	14°52'54"	39°55'37"	Pool	Alid	515	36
ELW96-7	12-Feb	As'ela #1	n.m.	n.m.	Pool	Alid	480	54
ELW96-8	12-Feb	As'ela #2	n.m.	n.m.	Pool	Alid	480	57
ELW96-9	14-Feb	Ilegedi #3	14°52'54"	39°55'37"	Pool	Alid	515	66
ELW96-10	17-Feb	Humbebet	14°52'40"	39°53'52"	Seep	Alid	480	<60
<i>Gases</i>								
ELG96-1	07-Feb	Hulma	14°53'40"	39°54'20"	Fumarole	Alid	225	77
ELG96-2	08-Feb	Darere	14°52'41"	39°54'51"	Fumarole	Alid	580	95
ELG96-3	10-Feb	Ilegedi #1	14°52'54"	39°55'37"	Fumarole	Alid	515	95
ELG96-4	11-Feb	As'ela	n.m.	n.m.	Fumarole	Alid	480	95
ELG96-5	14-Feb	Ilegedi #3	14°52'54"	39°55'37"	Bubbling pool	Alid	515	84
ELG96-6	16-Feb	Abakri	14°53'22"	39°54'19"	Fumarole	Alid	485	94

n.m. is not measured. Latitudes measured relative to WGS84 datum. Elev. is elevation above mean sea level.

Eastern Lowlands, including the Danakil Alps region, and on the Eritrean highlands to the west of Alid. The chemical compositions of these waters are presented in Table 2.

The groundwaters and surface waters of Eritrea demonstrate great diversity: the Eritrean highland waters have total dissolved solids (TDS) generally in the range of 300 to 700 mg/l; the anions are mainly bicarbonate. In contrast, Afar/Eastern lowland waters tend to be relatively rich either in chloride or sulfate and the TDS content of well waters used for drinking ranges from ~600 to 5,600 mg/l (Table 2). Though some samples appear to have a seawater component, the dissolved solids in many eastern lowland groundwaters also can be attributed to dissolution of sulfate and halide salts that are present in Tertiary marine sediments.

Partial analyses from an earlier survey of the region (Beyth, 1994) are also shown in Table 2 (*MB #*). Samples from Gelti and Gerba'naba, saline hot springs that emerge at the shore of the Gulf of Zula (ELW96-2 and -3), are listed for completeness in Tables 1 and 2, and shown in Fig. 3, but are not discussed further and are not considered strictly relevant to the geothermal system at Alid because of their immediate proximity to the sea and obvious seawater-influenced compositions. Nevertheless, fluids with relatively high TDS may be present beneath Alid, given the likely presence of marine evaporites in the subsurface of the Danakil depression and the former presence of the Red Sea in this region, prior to 32 ka (Bonatti et al., 1971). High-temperature (~255°C) geothermal fluids from the Asal geothermal field in Djibouti (Fig. 1) have high TDS (~13 wt.%) and compositions consistent with leaching of marine evaporites (Correia et al., 1985).

5.2. Isotopic composition

Table 2 includes results of isotopic analyses for meteoric waters collected from shallow wells and streams in the eastern lowland and central highland regions of Eritrea. The data are plotted in Fig. 4, along with the trend for meteoric waters throughout the world (Craig, 1961). Most of the Eritrean meteoric waters plot along a 'local' trend slightly above the world average meteoric water line. The most important observation is that all of the meteoric waters collected in the central highlands are isotopically lighter (more negative values) than the meteoric waters collected in the Eastern Lowlands. These results are expected, given the regional rainfall patterns and topographic relief. Lowland rains are produced from clouds coming from the northeast, off the Red Sea. Because the Red Sea itself is partially evaporated, and contains δD values greater than VSMOW by up to +9‰ (Craig, 1966, 1969), rains derived from the Red Sea should also be high in δD . In contrast, summer rains in the Eritrean highlands come from storms that have swept across Africa from the Atlantic Ocean, which has a composition approximately that of VSMOW. The long travel distance of such storms and the high elevation of the Eritrean highlands result in precipitation that has lower values of δD (Craig, 1961).

Table 2. Chemistry and isotopic composition of Eritrean ground waters, surface waters and steam condensates

Sample no	Name	Temp. (°C)	pH field	pH lab	Cond. (μS/cm)	TDS (mg/l)	SiO ₂ (mg/l)
<i>Regional Waters</i>							
ErF96-1	Kedra Village	30	7.0	7.84	3760	2602	43.0
ErF96-2	Irafayle	34	4.0	7.61	668	570	51.1
ErF96-3	Bordele	35	7.5	7.86	3790	2552	101
ErF96-4	Ghela'elo	35	6.8	7.42	1302	1077	110
ErF96-5	Akilo	30	7.5	7.55	8750	5584	87.9
ErF96-6	Gorei	38	7.5	8.05	2290	1739	81.5
ErF96-7	Adeto	37	7.5	7.73	2690	1921	91.6
ErF96-8	Boleli	34	7.0	7.74	1357	1048	43.6
ErF96-9	Boleli area	34	7.0	7.98	1667	1110	34.9
ErF96-10	Adi Ela	38	7.0	7.89	872	701	78.7
ErF96-11	Somoti	36	7.5	7.63	6110	3730	75.9
ErF96-12	Near Gahtielay	42	7.5	8.18	1033	905	73.2
ErF96-13	Simoli	24	6.3	7.93	393	337	21.4
ErF96-14	Zegfel (NE of Simoli)	24	6.5	8.03	668	552	18.5
ErF96-15	Near border with Ethiopia	28	6.5	7.92	631	468	18.2
ErF96-16	Adi-Keyh	28	6.5	8.02	646	560	20.9
ELW96-1	Rain near Boya	est 30					
ELW96-2	Gelti hot spring	58	7.0	7.23	15080	9089	116
<i>MB 1</i>	<i>Gelti hot spring area</i>	<i>est 60</i>				<i>14633</i>	<i>125.0</i>
<i>MB 1a</i>	<i>Gelti hot spring area</i>	<i>est 60</i>				<i>15029</i>	<i>125.0</i>
<i>MB 2</i>	<i>Gelti hot spring area</i>	<i>est 60</i>				<i>14802</i>	<i>124.0</i>
<i>MB 3</i>	<i>Gelti hot spring area</i>	<i>est 60</i>				<i>14776</i>	<i>126.0</i>
ELW96-3	Gerba'naba hot spring	54	7.0	7.28	24400	15176	121
ELW96-4	Boya Well	33		7.86	1458	1229	56.7
<i>MB 7</i>	<i>Boya well</i>					<i>766</i>	<i>63</i>
<i>MB 8</i>	<i>Boya well</i>					<i>764</i>	<i>65</i>
<i>MB-9</i>	<i>Boya well</i>					<i>1224</i>	<i>56</i>
ELW96-11	Boya well	33	—	8.13	1448	1195	54.3
ELW96-12	Alad Stream		8.0	8.05	7890	7258	82.6
ELW96-13	Kusurale well	36	7.0	7.58	2610	1572	86.9
<i>Alid Hydrothermal Waters</i>							
ELW96-5	Ilegedi No 1 pool	50	5.0	3.34	2450	1695	195
ELW96-6	Ilegedi No 2 pool	35	3.0	2.31	4260	2606	402
<i>MB 4</i>	<i>Pool in Ilegedi vicinity</i>					<i>354</i>	<i>140</i>
<i>MB 4A</i>	<i>Pool in Ilegedi vicinity</i>					<i>731</i>	<i>140</i>
<i>MB5</i>	<i>Pool in Ilegedi vicinity</i>					<i>323</i>	<i>200</i>
<i>MB 6</i>	<i>Pool in Ilegedi vicinity</i>					<i>833</i>	<i>120</i>
ELW96-7	As'ela No 1 pool	54	7.0	7.50	2770	2417	114
ELW96-8	As'ela No 2 pool	57	7.0	7.59	2050	1748	71.0
ELW96-9	Ilegedi No 3 pool	66	6.0	7.44	2230	1633	99.1
ELW96-10	Humbebet drip	<60	7.0	7.54	703	572	39.8
ELG96-2	Darere steam condensate	95	5.0	6.53	368	255	4.77
ELG96-6	Abakri steam condensate	94	5.0	6.74	291	204	2.27

Note: Analytical methods and errors discussed in Trujillo et al. (1987). MB samples (*in italics*) from Beyth (1994).

The disagreement between cation and anion sums for ELW96-6 may be due to the presence of hydrogen ion in this acid sample.

* Sample ELW96-10 was collected as two bottles from adjacent seeps. One bottle was analyzed for cations and the other for anions. Differences in bulk composition of the seeps may account for the disagreement between cation and anion sums.

† Summations in units of milli-equivalents per liter.

Sample no	Na (mg/l)	K (mg/l)	Ca (mg/l)	Mg (mg/l)	Li (mg/l)	Sr (mg/l)	NH ₄ (mg/l)	NO ₃ (mg/l)	Fe (mg/l)	Mn (mg/l)
<i>Regional Waters</i>										
ErF96-1	508	9.4	134	122	0.02	2.41	0.07	120	<0.01	<0.01
ErF96-2	71.1	20.0	42.6	7.60	<0.01	0.37	0.1	58.9	<0.01	<0.01
ErF96-3	713	12.7	59.9	31.4	0.03	1.58	0.05	18.4	<0.01	0.20
ErF96-4	47.6	10.5	146	57.9	0.01	4.50	0.09	25.3	0.05	<0.01
ErF96-5	841	13.2	936	59.0	0.01	15.4	0.14	0.04	0.14	1.14
ErF96-6	330	3.9	87.4	76.3	0.02	2.04	0.04	37.0	0.14	<0.01
ErF96-7	376	5.0	150	48.9	0.03	2.42	0.15	59.2	<0.01	<0.01
ErF96-8	89.4	17.0	147	39.2	<0.01	2.45	0.06	36.0	<0.01	0.16
ErF96-9	164	16.7	101	53.3	0.05	1.99	0.04	6.70	<0.01	<0.01
ErF96-10	61.8	3.7	80.9	25.3	<0.01	1.12	0.04	20.3	0.29	0.02
ErF96-11	880	59.7	272	79.8	0.13	4.49	0.23	29.3	0.03	1.55
ErF96-12	230	12.0	18.4	0.81	0.04	1.19	0.03	0.19	0.01	0.07
ErF96-13	19.3	3.0	39.7	14.5	0.01	0.18	0.11	7.92	2.36	0.05
ErF96-14	45.7	0.7	77.4	14.5	<0.01	0.45	0.03	47.0	0.03	<0.01
ErF96-15	15.7	32.2	63.7	16.3	<0.01	0.28	0.03	58.4	0.49	0.17
ErF96-16	25.6	0.3	81.8	25.6	<0.01	0.24	0.04	<0.02	0.06	<0.01
ELW96-1										
ELW96-2	2,320	120	940	88.8	0.60	19.9	0.06	54.3	<0.01	<0.01
MB 1	3,540	200	1640	145		38.0				
MB 1a	3,600	201	1640	150		38.0				
MB 2	3,580	203	1650	157		38.0				
MB 3	3,600	200	1620	146		39.0				
ELW96-3	3,640	192	1660	153	1.25	35.8	0.03	52.6	<0.01	<0.01
ELW96-4	73.5	33.2	142	73.5	0.05	1.90	0.04	38.6	0.08	<0.01
MB 7	59	32.0	150.0	82.0		2.4				
MB 8	59	32.0	150.0	80.0		2.3				
MB-9	59	32.0	150.0	78.0		2.4				
ELW96-11	69.7	32.7	126	73.9	0.10	1.90	0.10	39.8	<0.01	<0.01
ELW96-12	826	106	496	642	0.14	9.63	0.08	2.34	<0.01	0.02
ELW96-13	375	40.1	119	13.3	0.14	2.12	0.51	44.6	0.25	0.74
<i>Alid Hydrothermal Waters</i>										
ELW96-5	18.2	11.4	101	31.2	0.02	0.16	213	14.6	10.1	3.11
ELW96-6	18.3	132	114	23.5	0.02	0.39	105	17.6	19.7	3.20
MB 4	11	7	96	19.0		0.60				
MB 4A	11	7	96	19.0		0.70				
MB5	17	10	47	39.0		0.20				
MB 6	17	11	400	64.0		1.30				
ELW96-7	233	20	396	27.2	0.05	2.94	15.9	11.3	0.04	0.56
ELW96-8	213	17	251	21.7	0.04	3.04	5.80	13.0	0.17	0.24
ELW96-9	11.4	12	157	37.4	0.02	0.44	190	<0.02	0.82	3.04
ELW96-10	2.86	1.18	111	10.2	<0.01	0.06	30.4	30.9	<0.01	<0.01
ELG96-2	0.06	0.06	0.05	0.02	0.06	<0.01	59.6	<0.02	0.01	<0.01
ELG96-6	0.23	0.11	0.5	0.03	<0.01	<0.01	47.4	<0.02	<0.01	<0.01

Cl (mg/l)	SO ₄ (mg/l)	CO ₃ (mg/l)	HCO ₃ (mg/l)	F (mg/l)	B (mg/l)	Br (mg/l)	Cations (Sum [†])	Anions (Sum [†])	δD (‰)	δ ¹⁸ O (‰)
747	608		302	0.77	0.43	4.98	39.03	40.47	−9	−2.8
42	25.5		245	0.16	0.20	0.34	6.55	6.72	−2	−2.1
841	218		548	1.80	1.36	3.92	36.87	37.48	−1	−1.9
73	496		102	2.77	0.24	0.25	14.49	14.59	4	−1.4
2457	901		258	2.86	1.52	9.13	88.40	91.59	0	−1.4
245	514	23.4	334	1.93	1.10	0.94	25.11	24.53	4	−1.0
396	597		190	2.31	1.22	1.07	28.01	27.71	−1	−1.0
126	343		202	0.50	0.37	1.25	14.93	14.60	2	−1.5
285	299		144	0.37	0.33	2.89	17.02	16.72	1	−0.7
97	85.7		245	0.53	0.21	0.21	8.94	8.88	1	−1.4
1700	422		186	2.45	1.10	15.7	59.92	60.05	−2	−2.0
71	78.3	19.5	393	6.48	0.25	0.38	11.32	11.05	−9	−3.3
17	12.8		198	0.15	0.03	0.15	4.23	4.14	−11	−3.5
29	28.7	15.4	274	0.13	0.11	0.34	7.07	7.19	−9	−3.2
50	49.0		163	0.08	0.06	0.36	6.07	6.03	−7	−2.8
14	40.5	19.0	332	0.26	0.06	0.21	7.32	7.32	−7	−2.5
									12	−1.4
5134	216		30	2.87	1.55	45.2	157.00	149.00	0	−1.6
8900			45							
9000	240		35							
9000			50							
9000			45							
8945	267		29	1.97	2.21	74.8	256.00	255.00	−7	−2.3
68	456	14.7	269	0.94	0.33	0.51	17.22	16.96	−4	−2.2
78			300							
76			300							
77	460		310							
59	458	20.0	258	0.99	0.33	0.41	16.28	16.77	−7	−2.2
687	4107	28.7	265	0.26	1.21	3.67	115.63	109.32	−1	−0.6
714	32.2		134	2.99	0.32	6.00	24.47	23.79	7	−0.6
2.99	1094		0	0.45	0.022	0.02	21.12	23.06	51	9.7
1.19	1767		0	0.21	0.031	<0.02	23.64#	37.00#	30	3.9
			80							
3	380		75							
10			20							
10			210							
20.9	1475		100	0.49	0.049	0.05	33.55	33.03	33	3.2
12.4	1068		66	0.43	0.044	0.05	24.39	23.93	35	3.6
0.84	949		171	1.18	0.015	<0.02	22.39	22.59	24	4.4
0.14	74.3		263	0.04	<0.002	<0.02	8.22*	6.53*	12	−0.9
0.07	1.71		189	0.03	0.002	<0.02	3.32	3.14	10	−4.0
0.07	0.55		153	0.05	<0.002	<0.02	2.67	2.52	−1	−2.8

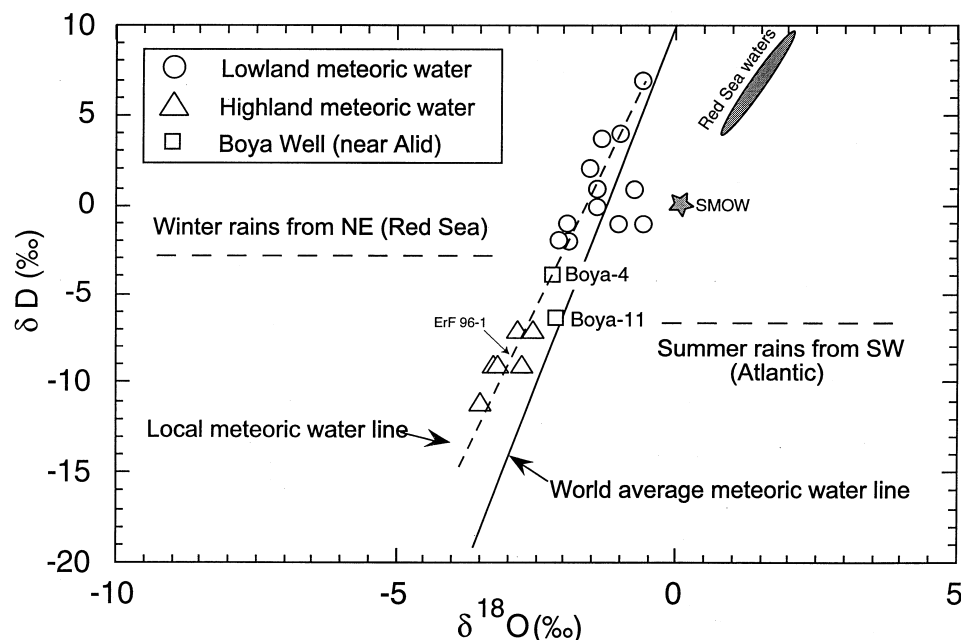


Fig. 4. Stable isotope variation diagram for $\delta^{18}\text{O}$ and δD in units of per mil (‰) relative to VSMOW. Waters from the highlands (triangles) clearly plot well below those from the Eastern lowlands, presumably due to their origin as summer rains off the Atlantic Ocean, rather than from the Red Sea. Sample ErF96-1 is grouped with the highland waters because it, like the Boya waters, comes from an alluvial fan draining the highland. The thermal waters from Gelti and Gerba'naba are not plotted, nor is the winter rainwater collected near Boya (ELW96-1). The range for summer and winter rains are interpreted, based on discussion in the text. Red Sea waters from Craig (1966, 1969).

6. Geothermal manifestations of Alid volcanic center

With the help of local inhabitants, we identified eleven geothermal sites on Alid volcanic center. We visited nine and selected six as suitable for sampling of gas and water emanations (Fig. 2; Tables 1, 2 and 3). Darere, Ilegedi and As'ela (Fig. 5a) are the most prominent vent areas, and of these Ilegedi is the largest and most active. Samples of fumarolic gases and steam were obtained from these three areas and from Abakri and Hulma. All sampled vent areas, except Hulma, contained fumaroles with temperatures at or just below the boiling point for their elevation. Fumarolic vents at Humbebet were too narrow to sample, and we instead collected water from seeps located adjacent to the fumaroles. We also sampled waters from thermal pools at As'ela and Ilegedi (Fig. 5b), which are interpreted to be evaporated mixtures of condensed fumarolic steam and shallow groundwater. Ghinda, Docholo and Dibara (Fig. 2) were not sampled due to their lack of vigorous fumarolic venting, but contained hot, steaming ground up to 93°C, 90°C, and 80°C, respectively. We were told of two other areas with steaming ground, Airole and Asgolo, but did not visit them. Two other localities near Alid may also have thermal features. During an

Table 3. Gas geochemistry of Alid fumaroles

Sample No [^]	ELG96-2	ELG96-3	ELG96-4	ELG96-5	ELG96-6
Location	Darere	Ilegedi No 1	As'ela	Ilegedi No 3	Abakri
Temp. (°C)*	95	95	95	84 (gas from bubbling pool)	94
CO ₂ (mol%) ^s	97.93	95.53	98.20	95.89	98.86
H ₂ S (mol%)	0.219	0.876	0.749	0.662	0.143
H ₂ (mol%)	1.093	2.498	0.503	2.624	0.605
CH ₄ (mol%)	0.225	0.132	0.061	0.144	0.085
NH ₃ (mol%)	0.128	0.389	0.004	0.005	0.095
N ₂ (mol%)	0.412	0.598	0.473	0.653	0.209
O ₂ (mol%)	0.0023	nd	nd	nd	0.0005
Ar (mol%)	0.0054	0.0126	0.0116	0.0140	0.0047
He (mol%)	0.00151	0.00047	0.00046	0.00073	0.00018
N ₂ /Ar	76.2	47.6	40.8	46.7	44.4
Gas/steam [†]	0.0448	0.0196	0.0259	1.701	0.0565
δD ‰ VSMOW	10	5	5	n.a.	−1
δ ¹⁸ O ‰ VSMOW	−4.0	−0.9	−1.7	n.a.	−2.8
δ ³⁴ S ‰ CDT	−1.7	0.9	2.0	2.0	1.3
δ ¹³ C ‰ VPDB	−3.4	−3.4	−4.9	−3.3	−3.3
T Calc (DP) °C [@]	218	266	225	262	206
T Calc (H-Ar) °C	336	336	290	334	323

n.d. not detected; n.a. not applicable

[^] ELG96-1 (Hulma; not listed) sampled at 77°C and contained ~97% air. Composition in Duffield et al. (1997).

* ELG96-2,3,4,6 were boiling-temperature fumaroles with no superheat. Temperature readings may be ~2°C lower than actual conditions.

^s Gas concentrations in mole % of dry gas.

[†] Gas/steam ratio is moles total non-condensable gas divided by moles H₂O.

[@] T Calc rows represent temperatures calculated with D'Amore and Panichi (DP:1985) and H₂/Ar (Giggenbach and Goguel, 1989) geothermometers. See text for details.

expedition in 1901–02 (Marini, 1938; translated in Lowenstern and Villa, 1998), fumaroles were observed at M. Gadahehi, a rhyolitic center in frhy3, about 4 km east of the summit of Alid, and at Assagaro ~10 km southeast of the summit of Alid in the southern 'Oss' basalt (yb). Neither locality was visited for this study.

Fumaroles and boiling pools are distributed widely on the north half of Alid, suggesting that a hydrothermal system underlies at least 10 km². Fumaroles vent through rhyolite breccia (Abakri, As'ela, Darere), the sedimentary sequence (Humbebet), and Precambrian basement rocks (Ilegedi). Therefore, their location does not appear to be controlled by lithologic type or contacts of different lithologic units. Most of the thermal manifestations are located at elevations between about 460 and 600 m, though hot rock and steaming vents also are present as low as 225 m (Hulma) and slightly higher than 760 m (Airole).

Some fumaroles are aligned, suggestive of fault control. For example, several areas

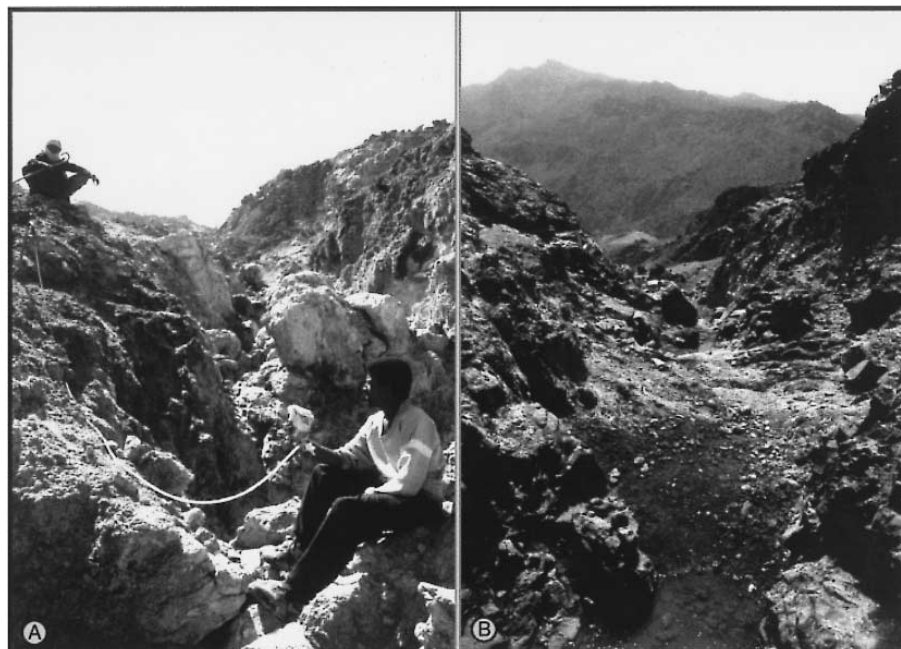


Fig. 5. Photos of thermal sites of Alid volcanic center. A) Sampling fumarolic vent at As'ela, a thermal area within a ravine on the steep north flank of Alid. The nearby rock is hydrothermally altered and contains surface deposits with abundant sublimates of sulfates. B) An acid thermal pool (~ 1 m across) at Ilegedi, where fumarolic steam condenses and mixes with shallow groundwater.

of alteration, including the one at Hulma, lie in a N50E zone, parallel to the north base of Alid. Abakri, As'ela and Humbebet occur in adjacent drainages on the north flank of Alid along a roughly N45E trend. These alignments may be associated with radial and concentric fractures formed during emplacement of the structural dome (Fig. 6 of Duffield et al., 1997). Thermal areas do not occur within the flat pumice-covered areas in the summit depression, perhaps because any fluids ascending there become diluted by local groundwater and laterally disseminated by the thick deposits of porous, reactive pumice before reaching the surface. Possibly for the same reason, fumaroles are absent in the porous young basalts to the north of Alid.

The sublimates and alteration minerals surrounding the fumarole vents are broadly similar in the various thermal areas. White and red clays, white and yellow crustose sublimates, and fine-grained white and green sublimates are ubiquitous. Beyth (1994, 1996) found that some of the sublimate minerals are ammonium hydrates and sulfates. We identified anhydrite (CaSO_4), kalinite/alum [$\text{KAl}(\text{SO}_4)_2 \cdot 11\text{H}_2\text{O}$], tschermigite [$(\text{NH}_4)\text{Al}(\text{SO}_4)_2 \cdot 12\text{H}_2\text{O}$], montmorillonite and illite among the alteration minerals at fumaroles. Tschermigite and alum are salts that form where ammonium- and sulfate-bearing waters react with crustal rocks at sub-boiling temperatures and oxidizing atmospheric conditions. These minerals precipitate as solutions evaporate, leaving crustose deposits or efflorescences (Dunning and Cooper, 1993). The relatively high

ammonium, calcium, potassium and sulfate concentrations in the pools are consistent with such an origin.

6.1. *Chemistry of thermal pools*

The thermal pools at Alid all have relatively high total dissolved solids (TDS ~1500–2500 mg/l, Table 2) and some are mildly acidic. Their compositions are strongly affected by dissolution of the surrounding host rock by sulfuric acid derived from the rising fumarolic vapor and gases. This results in the formation of clay minerals after feldspars, and release of cations to solution. The acidic Ilegedi samples contain far more dissolved silica than the less-acidic As'ela waters. The differences in acidity and composition may in part reflect the small differences in gas compositions but could also be due to reaction between wallrock and vapor in the shallow subsurface. The water collected at Humbebet was sampled directly from a seep; its composition is similar to that of direct steam condensates from the fumaroles. It appears to have undergone relatively little evaporation or reaction with surface rocks.

Because the Alid thermal pools are highly evaporated, as shown by the isotopic data discussed below, and because their dissolved components appear to reflect late-stage reaction between steam condensate and surface rocks, the chemical compositions of these 'acid sulfate' pools differ greatly from fluid compositions in the 'parent' geothermal reservoir beneath Alid. The compositions of neutral-chloride waters and other fluids typical of hot-spring environments are often used as indicators of subsurface temperatures (e.g., Chapter 3 of Henley et al., 1984). At Alid, such fluids have not been found, quite likely because the regional groundwater table is below the graben floor. Fumarolic gases, however, can ascend through the unsaturated zone to vent on the summit and flanks of Alid.

6.2. *Noncondensable gas compositions*

Analyses of gas samples from Alid fumaroles are listed in Table 3. All of the samples contained over 95% steam, with the exception of the boiling pool of Ilegedi #3 where most of the steam condensed in the pool and consequently could not be collected. Because the fumarole samples were not superheated with respect to their atmospheric venting temperatures (all about 95°C or less), some steam may have condensed as the vapors rose through the mountain. Gas/steam ratios shown in Table 3, therefore, may be much higher than those of deeper, hotter parent fluids (especially Ilegedi #3, from a boiling pool).

With the exception of Hulma, most of the Alid fumaroles have roughly similar gas compositions (Table 3) and insignificant air contamination, as indicated by oxygen concentrations generally near or below the detection limit. The high O₂ and N₂ of Hulma indicated that over 97% of this sample, discharged from a relatively cool vent at ~77°C, was moist air. As'ela was air-free, but was also slightly unusual in its low NH₃ and CH₄ concentrations. The thermal pools at As'ela also contained considerably less NH₃ than those at Ilegedi. This could result from a lower input of NH₃ derived from decomposition of organic materials in marine sediments at depth. However, this

explanation is not consistent with the observation that As'ela is located within the 'sedimentary sequence,' whereas Ilegedi, with higher methane and ammonia concentrations, vents directly from the basement schists. Most probably, the steam vented at As'ela traverses a greater amount of saturated or partly saturated ground before reaching the surface, allowing NH_3 to be absorbed by shallow groundwater.

In spite of the variations in minor gas constituent abundances, similarities among the Alid fumaroles were more notable than differences. The non-condensable gas compositions of all samples range from 95.5–99 mol% CO_2 , and H_2 is generally the next most abundant component (0.5–2.5 mol%).

The N_2/Ar ratio for the fumarole gases generally ranges from 41 to 48, similar to a value of 38 for air-saturated water (Fig. 6). Within geothermal systems, the oxygen in air-saturated groundwater is removed by reaction with rocks at high temperature, whereas N_2 , Ar, and He remain relatively unchanged. In Fig. 6, all data fall on a trend from air-saturated water toward He-rich and CO_2 -rich components. The Darere fumarole is especially enriched in He, which may come from radioactive breakdown of the Precambrian granites and schists or, more likely, is provided by mantle input

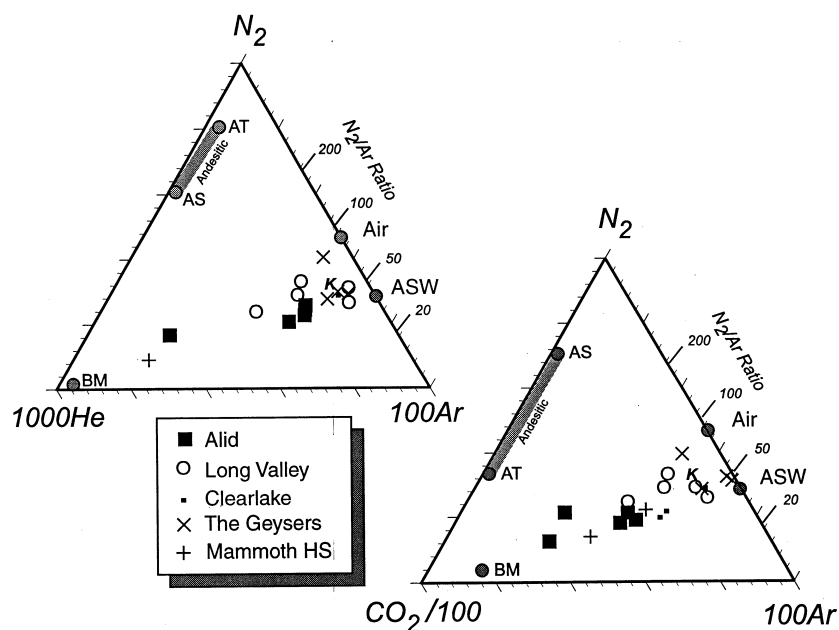


Fig. 6. Triangular diagrams of N_2 vs. 1000He vs. 100Ar and N_2 vs. $\text{CO}_2/100$ vs. 100Ar for fumarolic samples from the Alid volcanic center. Fumaroles from other non-arc-hosted geothermal systems are plotted for comparison and their gas compositions are listed in Table 4. The samples trend from an endmember of air-saturated groundwater (ASW) contaminated with air toward a mantle-endmember composition. The endmembers for basaltic mantle (BM), andesitic subducted (AS) and andesitic thermogenic (AT) are from Giggenbach (1992). The AT component is believed to be added to andesitic magmas by interaction with heated sedimentary crustal materials. The value for the Olkaria system in Kenya (symbol = K) is for downhole samples from Giggenbach (1992).

in the form of basaltic magmas underlying Alid. The data in Table 3 and Fig. 6 imply that the Alid fumaroles consist of steam and gas boiled from a geothermal fluid that is derived from groundwater that has been heated, has reacted with rock and has been enriched in gases of crustal and magmatic origin.

6.3. Gas geothermometry

Many studies have shown that residence times for gases within high-temperature geothermal systems typically are sufficient to allow attainment of chemical equilibrium. Initially, the gases are dissolved in liquid and escape along with steam during phase separation/boiling. Cooling occurs both adiabatically as a result of decompression, and by conduction as the vapors rise toward the earth surface. During relatively rapid upflow and cooling, most gases re-equilibrate slowly, so that they retain the chemical speciation previously attained at higher temperature. Gas geothermometers make use of this relict speciation to estimate the initial temperature of the deeper system (Giggenbach and Goguel, 1989; Chapter 5 of Henley et al., 1984; Ping and Ármannsson, 1996).

In our past experience, we have found that the D'Amore and Panichi (1980) method, which utilizes the relative abundances of CH_4 , CO_2 , H_2S and H_2 , generally gives very reliable results. These particular gases have relatively low solubilities in water and, therefore, tend not to be greatly affected by condensation and interaction with hot or cold groundwaters. The D'Amore and Panichi (1980) geothermometer indicates temperatures of 265°C for Ilegedi, the largest and most active of the Alid geothermal manifestations. The abundance of methane is negatively correlated with the calculated geothermometer temperature, so that addition of organically derived methane in the shallow subsurface would cause the geothermometer to give temperatures that are lower than the actual temperature at depth.

Another commonly used gas geothermometer is the H_2/Ar method discussed by Giggenbach and Goguel (1989). As temperature increases, water is progressively dissociated, creating higher partial pressures of hydrogen. Argon is used to normalize the abundance of hydrogen, as it has a low solubility in water, similar to that of hydrogen, and is derived almost entirely from degassed, air-saturated groundwater. The H_2/Ar ratio therefore does not change significantly due to secondary processes such as condensation, mixing and boiling. Air contamination of a gas sample, if it were to occur, would result in high Ar concentrations and lower temperatures calculated by the H_2/Ar geothermometer. Instead, at Alid the H_2/Ar method yields high temperatures, ranging from 290 to 336°C.

Results acquired with the D'Amore and Panichi (1980) and H_2/Ar geothermometers are positively correlated both for the samples from Alid and those from other geothermal areas. In Fig. 7 and Table 4, we compare temperatures calculated by gas geothermometry for fumaroles and hot springs from The Geysers, California, Cerro Prieto, Mexico, the Clearlake region, California, Mammoth Hot Springs, Wyoming, and Long Valley Caldera, California. These geothermal areas have different subsurface temperatures, as shown by downhole measurements (see caption to Fig. 7). The two geothermometers predict reasonable reservoir temperatures. Notwithstanding

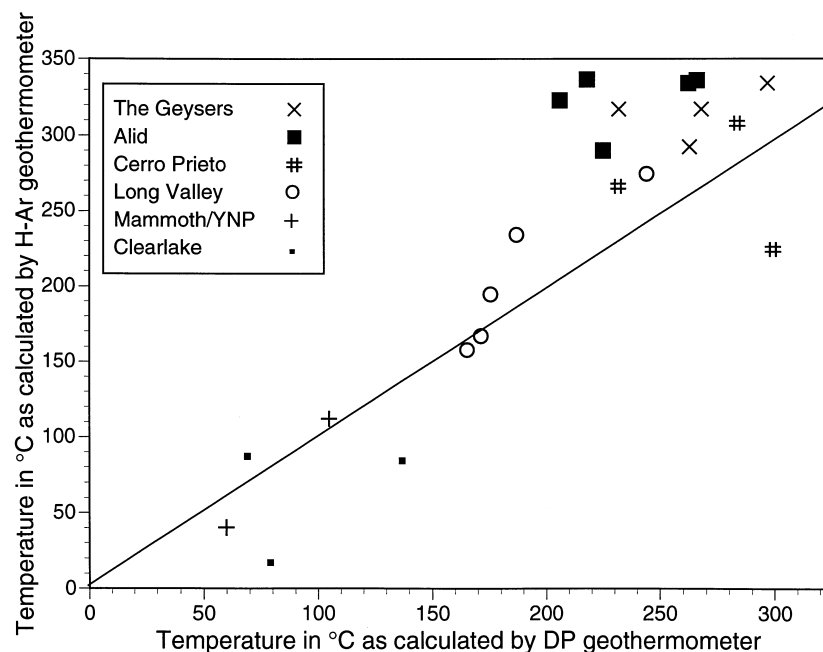


Fig. 7. Plot of temperature calculated using the H_2/Ar (H-Ar) geothermometer of Giggenbach and Goguel (1989) versus that calculated using the D'Amore and Panichi (1980) geothermometer (DP). Full analyses and references for each calibration sample are listed in Table 4. The Clearlake gas samples are from bubbling hot or cold springs with a strong component of formation water. Expected equilibration temperatures for the gases should be less than 140°C . Gases from the two hot springs at Mammoth, in Yellowstone National Park, come from a region of travertine terraces; solute geothermometers and measurements in shallow wells indicate initial temperatures of $80\text{--}100^\circ\text{C}$. The Long Valley samples come from fumaroles near the Casa Diablo geothermal power plant, which draws from a reservoir at $150\text{--}170^\circ\text{C}$. The Cerro Prieto and The Geysers gases come from fumaroles near these two large geothermal systems with downhole temperatures between 240 and 300°C . The diagonal line indicates the trend expected for a perfect 1:1 correlation for the two geothermometers.

the higher temperature predicted by the H_2/Ar geothermometer for the Alid high-temperature samples, one can clearly infer 'deep' temperatures by analysis of surface manifestations such as fumaroles and gas discharges from hot springs. Gas geothermometry of the Alid fumaroles thus indicates that the subsurface geothermal system is likely to be greater than $\sim 225^\circ\text{C}$.

6.4. Isotope geochemistry

6.4.1. Thermal pools and seeps

The isotopic compositions of thermal pools and steam condensates from Alid are listed in Table 3 and shown in Fig. 8. The waters collected from thermal pools, with one exception, are isotopically very heavy (δD up to $+51\text{‰}$) and plot below the world and local meteoric water lines. Their isotopic compositions likely result from

Table 4. Analyses of surface gas samples used to assess H₂/Ar and D'Amore-Panichi gas geothermometers.

Sample no.	Ref.*	Location	T (°C)	CO ₂ (mol %)	H ₂ S (mol %)	H ₂ (mol %)	CH ₄ (mol %)	NH ₃ (mol %)	N ₂ (mol %)	O ₂ (mol %)	Ar (mol %)	He (mol %)	T(DP) (°C)	T(H-Ar) (°C)
Casa Diablo 1/90	1	Long Valley, CA, USA	93	96.4	0.676	0.0266	0.0204	n.a.	2.33	0.0827	0.0472	0.00044	165	158
Casa Diablo 7/90	1	Long Valley, CA, USA	93	96.6	0.630	0.045	0.036	n.a.	2.39	0.044	0.059	0.00073	171	167
Casa Diablo 1/91	1	Long Valley, CA, USA	93	99.1	0.466	0.0922	0.0204	n.a.	0.76	0.120	0.0133	0.0011	187	234
Casa Diablo 6/91	1	Long Valley, CA, USA	93	97.6	0.369	0.0530	0.014	n.a.	1.88	0.642	0.028	0.0010	175	194
Casa Diablo 1/92	1	Long Valley, CA, USA	97	98.3	0.910	0.640	0.0197	n.a.	1.40	0.296	0.0244	0.0010	244	274
N-31	2	Cerro Prieto, Mexico	100.0	80.7	1.25	3.61	0.23	12.5	1.97	n.d.	0.046	n.d.	284	308
N-36	2	Cerro Prieto, Mexico	100.0	83.0	3.54	0.66	4.73	1.83	5.81	n.d.	0.13	0.00036	299	224
N-43	2	Cerro Prieto, Mexico	90.0	88.1	1.40	1.88	5.52	0.083	2.78	n.d.	0.094	n.d.	232	266
Clearlake 95-9	3	Wilbur Hot Spr., CA, USA	56.5	91.1	3.14	0.00107	4.88	0.00186	0.838	0.0033	0.0216	—	137	84
Clearlake 95-8	3	Grizzly Spring, CA, USA	21.5	98.0	0.0682	0.000115	1.20	0.00114	0.738	0.0066	0.0206	—	79	17
Clearlake 95-14	3	Horseshoe Spring, CA, USA	40.0	93.5	0.0043	0.00343	2.28	0.000935	2.9	1.24	0.0627	0.000976	69	87
GYS95-1 (2)	3	Old Geysers, CA, USA	40.5	83.6	2.19	5.22	6.57	0.00026	2.26	0.0159	0.0483	0.00109	268	317
GYS95-2	3	Hot Springs Cr., CA, USA	95.2	56.5	1.29	20.6	9.39	0.00039	9.40	3.17	0.191	0.00294	232	317
GYS95-4	3	L. Geysers Str., CA, USA	95.8	56.6	5.34	15.7	1.37	0.866	15.5	4.11	0.338	0.00363	263	292
G96-01	3	Fum., BSC rdmrk 2.51	~98	76.8	5.90	6.91	5.94	1.46	2.93	0.0139	0.0373	0.00057	297	334
Narrow Gauge	4	Mammoth HS, WY, USA	72	98.2	0.152	0.001	0.0036	n.a.	0.289	0.019	0.008	<0.0002	105	112
Snow Pass	4	Mammoth HS, WY, USA	8	98.6	0.0233	<0.0002	0.0462	n.a.	0.764	0.04	0.017	0.0059	60	40

DP = Geothermometer utilizing relative abundances of CH₄, CO₂, H₂ and H₂S from D'Amore and Panichi (1980). H-Ar = H₂/Ar geothermometer from Giggenbach and Goguel (1989).

* Refs: (1) Sorey et al. (1993); (2) Nehring and D'Amore (1984); (3) C. Janik (previously unpub. from Clearlake region and The Geysers, CA: manuscript in prep.); (4) Kharaka et al. (1991).

Significant figures as reported in original publication. n.a. not analyzed. n.d. not detected. Discussion of sampling sites is found in caption to Fig. 7.

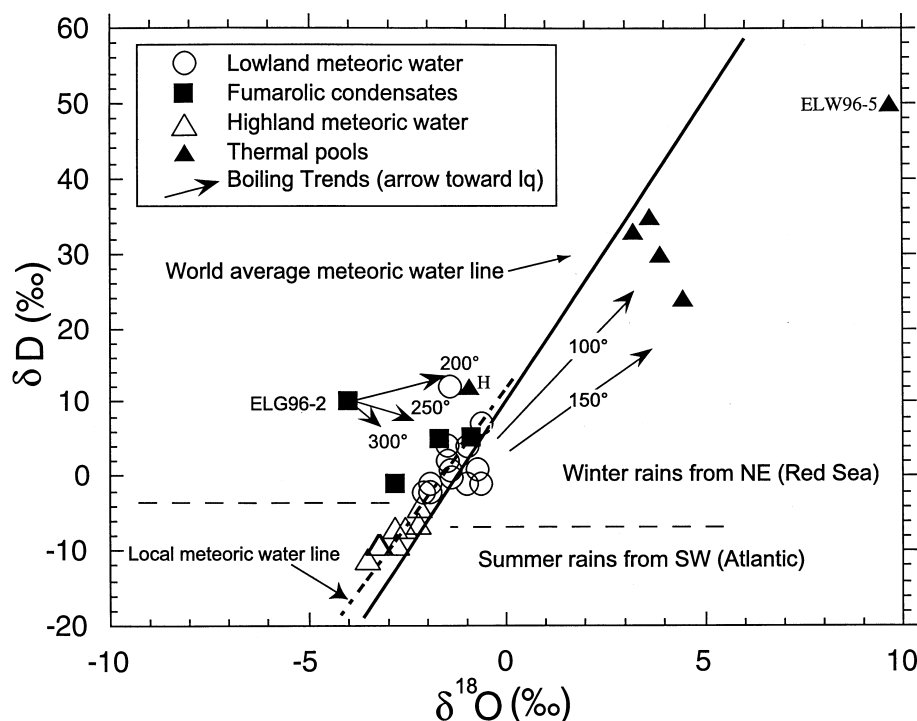


Fig. 8. Stable isotope compositions of Eritrean meteoric waters and hydrothermal fluids of Alid volcanic center. Vectors denote orientation and magnitude of fractionation due to boiling at various temperatures. Arrows point toward the liquid (see text). Thermal pools from Alid show evidence of evaporation at the surface. Fumarolic condensates most likely originated by boiling at $T > 220^{\circ}\text{C}$ from a geothermal fluid that originated as lowland meteoric waters and/or fossil Red Sea waters. In this diagram, Boya waters are plotted as highland waters, given their likely source region. Fields for winter and summer rains as in Fig. 4. Sample 'H' is ELW96-10 (Humbebet).

evaporation of relatively stagnant, hot ($50\text{--}90^{\circ}\text{C}$) bodies of water that are mixtures of local groundwater and steam condensate. Reaction of the relatively stagnant and sometimes acidic pool water with Precambrian wallrock would further shift the $\delta^{18}\text{O}$ of the water to higher values relative to the meteoric-water line. This might be a contributing factor in the attainment of the extremely high $\delta^{18}\text{O}$ values for one of the thermal pools from Ilegedi (Fig. 8; ELW96-5).

The sample collected at Humbebet (ELW96-10; labeled 'H' in Fig. 8) plots above the average world meteoric line and contains the lowest TDS of any of the thermal waters. Its chemical and isotopic composition is more similar to that of waters condensed directly from fumarolic steam than that of the thermal pools. In fact, the Humbebet sample was collected from a tepid seep rather than a hot evaporating pool. It may also have a large component of meteoric water, as its composition is remarkably similar to rain water that fell on Alid during the early morning of 5 February 1996 (ELW96-1: data point to left of H on Fig. 8).

6.4.2. Potential source waters for fumarolic steam

The isotopic compositions of condensed fumarolic steam show little evidence for significant incorporation ($> 10\%$) of magmatic or metamorphic waters, which would have $\delta^{18}\text{O}$ values $> 5\text{‰}$ and $\delta\text{D} < -20\text{‰}$ (Taylor, 1992). All Alid steam condensates have values close to, and slightly above, the local meteoric water line. This is not surprising, given that boiling hydrous solutions always produce steam that has a $\delta^{18}\text{O}$ value less than that of the coexisting liquid water (Craig, 1963). In contrast, the δD of steam is lower than that of coexisting liquid water only at temperatures $< 220^\circ\text{C}$. Above 220°C the δD of steam is higher than that of the coexisting boiling liquid (Friedman and O'Neil, 1977). In Fig. 8, arrows radiating from the datum for ELG96-2 (Darere) point to the location of potential coexisting boiling liquids at various temperatures. Steam separated from boiling liquid at temperatures lower than $\sim 200^\circ\text{C}$ could not produce ELG96-2 or the other Alid condensates (except possibly Abakri), as this would require reservoir waters with δD higher than any surface or groundwater identified in this study.

The relations shown in Fig. 8 indicate that the fumarolic steam most likely has derived from high-temperature ($> \sim 220^\circ\text{C}$) boiling of lowland meteoric water. The isotopic composition of the steam condensate also could have derived from a deep fluid that is fossil Red Sea water, recharged when the Red Sea previously filled the Danakil depression. The data indicate that the fumarolic steam could not have derived directly from a boiling fluid that is isotopically similar to highland meteoric water, which is too light in δD and $\delta^{18}\text{O}$. However, it is conceivable that the parent reservoir fluid is highland water that was previously evaporated at a low temperature (atmospheric conditions) before percolating underground.

6.4.3. Water-rock interaction

It would be useful to estimate the degree of water-rock interaction between the geothermal fluid and its host reservoir. If the water were relatively unreacted, it might indicate relatively high water/rock ratios, consistent with a permeable system. Unfortunately, it is difficult to assess whether the deep thermal waters are unreacted meteoric water or have undergone extensive water-rock interaction. The fractionation factors for feldspar/water and quartz/water exchange of oxygen isotopes are 9.6 and 12.2, respectively, at 200°C (Friedman and O'Neil, 1977). Therefore, geothermal waters that equilibrate completely with granitic rocks having $\delta^{18}\text{O}$ near $+8$ would be expected to have $\delta^{18}\text{O}$ somewhere between -2 and -4‰ . At this low latitude, meteoric waters already have compositions near these values and thus would not change appreciably in isotopic composition during water-rock interaction at 150 – 300°C with typical granitic rocks ($\delta^{18}\text{O}$ between 6 and 10‰). Though some local rocks have much higher values of $\delta^{18}\text{O}$ ('pc' mica schist, 18.2‰ ; 'pc' kyanite schist, 12.7‰ ; 'ss' siltstone 16.7‰ ; EC96-48, 41, and 17, respectively, from Duffield et al., 1997), other likely reservoir lithologies have values between 6 and 10‰ ('pc' granite, 8.9‰ ; 'ss' basalt, 9.1‰ ; 'pf' intrusive ejecta 6.6‰ ; EC96-44a, 18 and 25, respectively, from Duffield et al., 1997). Without information on the actual reservoir lithologies, it is difficult to estimate the degree of water-rock interaction.

6.4. Carbon and sulfur isotopes

Sulfur isotopes of H_2S from the Alid fumaroles are consistent with a magmatic source of sulfur to the geothermal system. Sampled values range from -1.7 to 2.0‰ $\delta^{34}\text{S}$ CDT (Table 4) and are consistent with those expected for mantle-derived sulfur (Taylor, 1986). Sulfur gases collected during an eruption at Erta Ale were found to be $\sim 1.0\text{‰}$ (Allard et al., 1977), and those from a rift eruption at Asal (Djibouti) were -2 to -3 (Allard, 1979). Given the low oxidation state of the Alid magmatic system (near quartz-fayalite-magnetite: Lowenstern et al., 1997), sulfur input to the system may be dominantly as H_2S , rather than SO_2 , and would result in H_2S with a distinctly magmatic/mantle S isotopic signature. Even if magmatic input were principally in the form of SO_2 , the H_2S formed by disproportionation of SO_2 in a reduced geothermal system would be similar in $\delta^{34}\text{S}$ to the original magmatic value (Kusakabe and Komoda, 1992). Sulfate produced via this reaction, and left dissolved within the liquid in the geothermal system, would be expected to have $\delta^{34}\text{S}$ that is 20 to 30‰ higher than the H_2S and original magmatic value (Ohmoto and Lasaga, 1982; Kusakabe and Komoda, 1992; Gamo et al., 1997).

Fumarolic sublimates range from 1.4 to 3.0‰ CDT, consistent with their formation from fumarole-derived sulfur. In contrast, sedimentary gypsum and anhydrite from the ‘sedimentary sequence’ are consistently high in $\delta^{34}\text{S}$, as is typical for sedimentary sulfate (Claypool et al., 1980). We obtained values of 10.9, 11.8 and 12.6‰ for two samples of gypsum and one of anhydrite, respectively, all from the ‘sedimentary sequence’. Because such values are much different from those observed in the Alid fumaroles, and because values of -1.7 to 3.0 are typical of granitic rocks, we suggest that sulfur input to the system is primarily magmatic.

The $\delta^{13}\text{C}$ of CO_2 in the Alid hydrothermal features varies from -3.3 to -4.9‰ VPDB, consistent with a magmatic source of CO_2 , possibly mixed with carbon from marine carbonate, which should be close to 0‰ or somewhat higher. The carbon isotopic composition of CO_2 from high-temperature volcanic gas of the Asal rift eruption, in the southern Afar, was measured at -5 to -6‰ VPDB (Allard, 1979); that from Erta Ale was $\sim -6\text{‰}$ (Allard et al., 1977). We conclude that most of the CO_2 and S emitted from Alid fumaroles is produced by degassing of the igneous body underlying Alid and its geothermal system.

7. Resource potential

The wide distribution ($\sim 10 \text{ km}^2$) of fumaroles on the northern half of Alid indicates that a relatively large heat anomaly exists beneath the volcanic center. Geological mapping and geochronology strongly link this heat source to a late-Pleistocene intrusion and related volcanism. The CO_2 , He and sulfur gases in the Alid fumaroles are likely to have derived from the underlying intrusion or due to regional magmatism. However, the presence of ammonia and methane in the fumaroles, and the temperatures inferred from gas geothermometry, clearly indicate that the fumarolic gas is boiled off a high-temperature geothermal system. The steam is not magmatic, but

has an isotopic composition consistent with boiling of regional groundwater. The chemical characteristics of the geothermal liquid are not known, but it could contain relatively high concentrations of TDS (> 10 wt.%), as at the Asal geothermal field in Djibouti, where groundwaters and related geothermal fluids have interacted with marine-derived sediments.

Given the lack of hot springs of deep origin on or around Alid (the acid-sulfate pools are derived from condensation of steam), any liquid-dominated geothermal reservoir is almost certainly located beneath the graben floor, 500 m or more beneath the depressed summit basin of Alid. It would reside well above the inferred heat source, a rhyolitic intrusion at ~ 4 km depth. Plausibly, the geothermal system could include an underpressured vapor-dominated reservoir, but it too would be located beneath the graben floor within a well-sealed wallrock carapace.

It seems possible that the subsurface beneath Alid is highly fractured and has sufficient permeability to make a viable geothermal field. Clearly, the deformation associated with ~ 1 km of late Pleistocene structural uplift would result in intense fracturing of the Precambrian wallrock and the overlying sedimentary and volcanic units. Subsequent eruption of numerous rhyolite lavas and pyroclastic flows would also cause brecciation of the rocks overlying the silicic magma chamber. Normal faulting and extension related to rifting of the Danakil depression would ensure that fractures are continually reactivated.

In summary, the geological and geochemical data from Alid geothermal system are favorable for further exploration and drilling. Future work should focus on identifying any zones of high heat flow and permeability that would serve as ideal sites for geothermal wells.

Acknowledgements

The authors would like to thank C. Kendall and W.C. Shanks III of the USGS for stable-isotope analyses, and D. Counce and F. Goff of Los Alamos National Lab for water-chemistry analyses. P. Lipman, F. Simon and M. Nathenson made the initial contacts that started this collaboration. T. Debrezion, H. Zerai and S. Baire of the Eritrean Ministry of Energy, Mines and Water Resources gave their continuing help and encouragement. The authors appreciate the inspired logistical efforts of A. Gartner and drafting by S. Priest. W.C. Shanks, P. Dobson, F. Goff and S. Ingebritsen provided helpful reviews. This project was funded in large part by the U.S. Agency for International Development, with additional support by the USGS Volcano Hazards Program and the Eritrean Ministry for Energy, Mines and Water Resources. The authors thank Unocal Corporation for permission to release data from The Geysers steam field.

References

- Allard, P., 1979. $^{13}\text{C}/^{12}\text{C}$ and $^{34}\text{S}/^{32}\text{S}$ ratios in magmatic gases from ridge volcanism in Afar. *Nature* 282, 56–58.

- Allard, P., Le Guern, F., Sabroux, J.C., 1977. Thermodynamic and isotopic studies in eruptive gases. *Geothermics* 5, 37–40.
- Bailey, R. A., Dalrymple, G. B., Lanphere, M.A., 1976. Volcanism, structure and geochronology of Long Valley Caldera, Mono County, California. *Journal of Geophysical Research* 81, 725–744.
- Barberi, F., Varet, J., 1977. Volcanism of Afar: Small-scale plate tectonics implications. *Geological Society of America Bulletin*, 88, 1251–1266.
- Beltrando, G., Camberlin, P., 1993. Interannual variability of rainfall in the Eastern Horn of Africa and indications of atmospheric circulation. *International Journal of Climatology* 13, 533–546.
- Beyth, M., 1994. A brief assessment of the Alid geothermal field: In: Report ES-10-94 of the Israel Ministry of Energy and Infrastructure. 11 pp.
- Beyth, M., 1996. Preliminary assessment of the Alid geothermal field, Eritrea. *Geological Survey of Israel Current Research*, 1996, 10, 124–128.
- Bonatti, E., Emiliani, C., Ostlund, G., Rydell, H., 1971. Final dessication of the Afar rift, Ethiopia. *Science* 172, 468–469.
- Claypool, G. E., Holser, W. T., Kaplan, I. R., Sakai, H., Zak, I., 1980. The age curves of sulfur and oxygen isotopes in marine sulfate and their mutual interpretation. *Chemical Geology* 28, 199–260.
- Clynne, M.A., Duffield, W.A., Fournier, R.O., Giorgis, L., Janik, C.J., Kahsai, G., Lowenstern, J., Mariam, K., Smith, J.G., Tesfai, T., 1996a. Geothermal potential of the Alid volcanic center, Danakil depression, Eritrea. U.S. Geol. Surv. Final Report to U.S. Agency for International Development under the terms of PASA Number AOT-0002-P-00-5033-00, 46pp.
- Clynne, M. A., Duffield, W. A., Fournier, R. O., Giorgis, L., Janik, C. J., Kahsai, G., Lowenstern, J., Mariam, K., Smith, J. G., Tesfai, T., 1996b. Geology and geothermal potential of Alid volcanic center, Eritrea, Africa. *Geothermal Resources Council Transactions* 20, 279–286.
- CNR-CNRS: Consiglio Nazionale delle Ricerche-Centre National de la Recherche Scientifique, 1973. Geology of northern Afar (Ethiopia). *Revue de Geographie Physique et de Geologie Dynamique* 15(4), 443–490.
- Correia, H., Fouillac, C., Gerard, A., Varet, J., 1985. The Asal geothermal field (Republic of Djibouti). In: Claudia Stone (Ed.) *International Symposium on Geothermal Energy*, Geothermal Resources Council Transactions International Volume 9(3), 513–519.
- Craig, H., 1961. Isotopic variations in meteoric waters. *Science* 133, 1702–1703.
- Craig, H., 1963. The isotopic geochemistry of water and carbon in geothermal areas. In: Tongiorgi E. (Ed.), *Nuclear Geology on Geothermal Areas*, Consiglio Nazionale delle Ricerche, Pisa, pp. 17–53.
- Craig, H., 1966. Isotopic composition and origin of the Red Sea and Salton Sea geothermal brines. *Science* 154, 1544–1548.
- Craig, H., 1969. Geochemistry and origin of Red Sea brines. In: Degens E.T., Ross, D.S. (Eds.) *Hot Brines and Recent Heavy Metal Deposits in the Red Sea*. Springer-Verlag, New York, pp. 208–242.
- D'Amore, F., Panichi, C., 1980. Evaluation of deep temperatures of hydrothermal systems by a new gas geothermometer. *Geochimica et Cosmochimica Acta* 44, 549–556.
- Duffield, W.A., Bullen, T.D., Clynne, M. A., Fournier, R.O., Janik, C.J., Lanphere, M.A., Lowenstern, J., Smith, J.G., W/Giorgis, L., Kahsai, G., W/Mariam, K., Tesfai, T., 1997. Geothermal potential of the Alid volcanic center, Danakil Depression, Eritrea. U.S. Geological Survey Open-File Report 97-291, 62pp.
- Dunning, G., Cooper, J.F. Jr., 1993. History and minerals of The Geysers, Sonoma County, California. *Mineralogical Record* 24, 339–354.
- Eklundh, L., Pilesjt, P., 1990. Regionalization and spatial estimation of Ethiopian mean annual rainfall. *International Journal of Climatology* 10, 473–494.
- Eritrea, Government of the State of (1995) Eritrea national map, 1:1,000,000.
- Fahlquist, L., Janik, C., 1992. Procedures for collecting and analyzing gas samples from geothermal systems. U.S. Geological Survey Open-File Report 92-211, 19pp.
- Food and Agriculture Organization, 1983. Assistance to land-use planning, Ethiopia: agroclimatic resources inventory for land-use planning. FAO, AG:DP/ETH/78/003, Technical Report 2.
- Friedman, I., O'Neil, J., 1977. Compilation of stable isotope fractionation factors of geochemical interest. In: Fleischer, M.K. (Ed.) *Data of Geochemistry*, 6th edition, U.S. Geol. Surv. Prof. Paper 440-KK.
- Gamo, T., Okamura, K., Charlou, J-L., Urabe, T., Auzende, J-M., Ishibashi, J., Shitashima, K., Chiba,

- H., and Shipboard Scientific Party of the ManusFlux Cruise, 1997. Acidic and sulfate-rich hydrothermal fluids from the Manus back-arc basin, Papua New Guinea. *Geology* 27, 139–142.
- Giggenbach, W.F., 1992. The composition of gases in geothermal and volcanic systems as a function of tectonic setting. In: Kharaka, Y.F., Maest, A.S. (Eds.), *Water-Rock Interaction, Proceedings WRI-7*, AA. Balkema, Rotterdam, pp. 873–878.
- Giggenbach, W.F., Goguel, R.L., 1989. Collection and analysis of geothermal and volcanic water and gas discharges. Report No. CD2401, New Zealand Department of Scientific and Industrial Research, 81pp.
- Henley, R. W., Truesdell, A. H., Barton, P.B. Jr., 1984. Fluid-mineral equilibria in hydrothermal systems. *Reviews in Economic Geology* 1, 267 pp.
- Kharaka, Y.K., Mariner, R.H., Bullen, T.D., Kennedy, B.M., Sturchio, N.C., 1991. Geochemical investigations of hydraulic connections between the Corwin Springs Known Geothermal Resources Area and adjacent parts of Yellowstone National Park. In: *Effects of potential geothermal development in the Corwin Springs Known Geothermal Resources Area, Montana, on the thermal features of Yellowstone National Park*. U.S. Geological Survey Water Resources Investigations Report 91-4052, F1-FX.
- Kusakabe, M., Komoda, Y., 1992. Sulfur isotopic effects in the disproportionation reaction of sulfur dioxide at hydrothermal temperatures. In: Hedenquist, J.W. (ed.), *Magmatic Contributions to Hydrothermal Systems*, Geological Survey of Japan Report 279, 93–96.
- Larson, P. B., Zimmerman, B.S., 1991. Variations in $\delta^{18}\text{O}$ values, water/rock ratios, and water flux in the Rico paleothermal anomaly, Colorado. *Geochemical Society Special Publication* 3, 463–469.
- Lowenstern, J.B., Villa, F. (eds. and translators), 1998. *Alid Volcano in the colony of Eritrea*, translation of: Marini, Angelo, 1938, *Il vulcano Alid nella colonia Eritrea*. *L'Universo* 19, pp. 51–65, 131–170: U.S. Geological Survey Open-File Report 98-218, 94 pp.
- Lowenstern, J. B., Clynne, M. A., Bullen, T.D., 1997. Comagmatic A-type granophyre and rhyolite from the Alid volcanic center, Eritrea, northeast Africa. *Journal of Petrology* 38, 1707–1721.
- Marinelli, G., Quaia, R., Santacroce, R., 1980. Volcanism and spreading in the northernmost segment of the Afar rift (Gulf of Zula). In: *Geodynamic evolution of the Afro Arabian rift system*, Accademia Nazionale dei Lincei, Rome, Atti dei Convegni Lincei, vol. 47, pp. 421–435.
- Marini, A., 1938. *Il vulcano Alid nella Colonia Eritrea*. *L'Universo* 19, 51–65, 131–170.
- Michael, A.H. 1986. The weather over Eritrea, in *Local Weather Prediction for the Red Sea Countries*. WMO Tropical Meteorology Research Progress Report 29, 45–55.
- Nehring, N. L., D'Amore, F., 1984. Gas chemistry and thermometry of the Cerro Prieto, Mexico, geothermal field. *Geothermics* 13, 75–89.
- Ohmoto, H., Lasaga, A.C., 1982. Kinetics of reactions between aqueous sulfates and sulfides in hydrothermal systems. *Geochimica et Cosmochimica Acta* 46, 1727–1745.
- Ping, Z., Ármannsson, H., 1996. Gas geothermometry in selected Icelandic geothermal fields with comparative examples from Kenya. *Geothermics* 25, 307–347.
- Smith, J.V., 1974. *Feldspar Minerals*, vol. 2, Chemical and Textural Properties. Springer-Verlag, New York, 690 p.
- Sorey, M.L., Kennedy, B.M., Evans, W.C., Farrar, C.D., Suemnicht, G.A., 1993. Helium isotope and gas discharge variations associated with crustal unrest in Long Valley Caldera, California, 1989–1992.
- Souriot, T., Brun, J.-P., 1992. Faulting and block rotation in the Afar triangle, East Africa: The Danakil crank-arm model. *Geology* 20, 911–914.
- Taylor, B.E., 1986. Magmatic volatiles: isotopic variation of C, H, and S. In: Valley, J.W., Taylor Jr., H.P., O'Neil, J.R., (Eds.) *Stable Isotopes in High Temperature Geologic Processes*, *Reviews in Mineralogy*, vol. 15, pp. 185–225.
- Taylor, B.E., 1992. Degassing of H_2O from rhyolite magma during eruption and shallow intrusion, and the isotopic composition of magmatic water in hydrothermal systems. In: Hedenquist, J.W. (Ed), *Magmatic Contributions to Hydrothermal Systems*, Geological Survey of Japan Report, vol. 279, pp. 190–194.
- Trujillo, P.E., Counce, D., Grigsby, C.O., Goff, F., Shevenell, L., 1987. Chemical analysis and sampling techniques for geothermal fluids and gases at the Fenton Hill Laboratory. Los Alamos National Lab Publication LA-11006-MS, 84pp.
- UNDP: United Nations Development Programme, 1973. *Investigations of the geothermal resources for power development*. Imperial Ethiopian Government, Ethiopia, 275pp.